Y. Fu, W. Zuo, M. Wetter, J. W. VanGilder, P. Yang 2019. "Equation-based object-oriented modeling and simulation of data center cooling systems." Energy and Buildings, 198, pp. 503-519. DOI: https://doi.org/10.1016/j.enbuild.2019.06.037.

Equation-based Object-oriented Modeling and Simulation of Data Center Cooling Systems

Yangyang Fu[a], Wangda Zuo[a,b,*], Michael Wetter[c], James W. VanGilder[d], Peilin Yang[a]

[a]Department of Civil, Environmental and Architectural Engineering, University of Colorado Boulder, Boulder, CO, USA;

[a]National Renewable Energy Laboratory, Golden, CO, USA;

[c]Lawrence Berkeley National Laboratory, Berkeley, CA, USA;

[d]Schneider Electric, 800 Federal Street, Andover, MA, USA;

*Corresponding author: Wangda.Zuo@colorado.edu

Abstract

In this paper, we introduce a newly developed open source data center package in the Modelica Buildings library to support modeling and simulation of cooling and control systems of data centers. The data center package contains major thermal and control component models, such as Computer Room Air Handler, Computer Room Air Conditioner, models of different subsystem configurations such as chillers with differently configured waterside economizers, as well as templates for different systems. Two case studies based on this package are performed to investigate the performances of the cooling and electrical system under normal conditions and emergency situations such as a blackout: one is for a data center powered by conventional energy,

and the other is for a data center powered by renewable energy. Simulation results show that the dynamic modeling and multi-domain simulation in the Modelica-based tool make it convenient for users to investigate both normal and emergent operations for conventional and renewable data centers.

Keywords: Equation-based Modeling, Waterside Economizer, Data Center, Emergency Operation

1 Introduction

Data centers are critical, energy-intensive infrastructures that support the fast growth of the information technology (IT) industry and the transformation of the economy at large. In 2010 data centers consumed about 1.1% to 1.5% of the total worldwide electricity and the number was about 1.7% to 2.2% for the U.S. [1]. The energy in data centers is mainly consumed by two parts: IT equipment (e.g., servers, storage, network, etc.) and infrastructure facilities (e.g., cooling system). The latter usually accounts for about half of the total energy consumption in a typical data center [2].

Modeling and simulation is a cost-effective way to evaluate the design and operation of cooling systems. Different physical systems (thermal, electrical, and electromagnetic, etc.) with different time-scaled dynamics are involved in such systems. This usually leads to differential algebraic equations. Simulation is then conducted to numerically solve the mathematical equations in order to calculate the system performance.

Many tools have been developed in academia and industry to perform computer modeling and simulation of cooling systems in data centers. For example, eQuest [3], EnergyPlus [4], [5], TRNSYS [6], and some customized simulation tools such as Energy Modeling Protocol [7] have

been used to study cooling systems with waterside economizers (WSE) and airside economizers (ASE) in data centers. Most of these traditional tools are based on imperative programming languages such as FORTRAN and C/C++. When implementing a physical model in these tools, model developers utilize their expertise to sort the physical equations in an order so that the unknowns (model outputs) in the equations can be solved based on given known variables (model inputs). The nonlinear equations are usually manipulated to be solved iteratively, and the differential equations are discretized to numerically approximate the state variables. Then, the model developers write the variable assignments into computer source codes. Other computer program procedures may be called in the source codes to calculate the input variables from a subsystem at each time step, which might request from the solver re-simulation of a subsystem iteratively [8].

The above-mentioned conventional simulation tools expose several disadvantages in terms of their modeling and simulation performance. First, in the imperative programming languages, mathematical equations are typically intertwined with numerical solvers. For example, a typical zone model is mathematically described as a first-order differential equation as shown in Eq.(1), where m is the zone air mass, $c_{p,a}$ is the specific heat capacity of the air, T_{zone} is the zone air temperature, t is time, and Q_i is the ith heat source in the zone.

$$mc_{p,a}\frac{dT_{zone}}{dt} = \sum_{i=1}^{n} Q_i(T_{zone}) \quad (1)$$

In EnergyPlus that is written in C++, the zone model is represented by discretizing the differential term on the left side over time. One of the discretization algorithm used for the zone model is the 3rd-order backward difference formula, which converts the differential equation into a set of

algebraic equations as shown in Eq.(2).

$$mc_{p,a}\frac{\frac{11}{6}T_{zone}^{t}-3T_{zone}^{t-\delta t}+\frac{3}{2}T_{zone}^{t-2\delta t}-\frac{1}{3}T_{zone}^{t-3\delta t}}{\delta t}=\sum_{i=1}^{n}Q_i(T_{zone}^{t}), \quad (2)$$

where δt is the length of the time step, and subscripts t,..., $t-3\delta t$ represent the time instance. The numerical method is integrated with the mathematical equations in the source codes, which leads to a program code that is hard to maintain. By accepting non-convergent solutions at intermediate time steps to the simulation results, the nested solver can also introduce numerical noises that can pose challenges to optimization programs [8]. Second, some platforms are not designed for evaluating the system dynamics and the semantics of their control have little in common with how actual control works [9]. For example, in EnergyPlus, the commonly used Proportional-Integral (PI) control loop is assumed to be ideal, i.e., there will be no overshoot. EnergyPlus also idealizes dead band or waiting time, which are frequently used in building controls. Moreover, many equipment models have built-in idealized control that requests flow rates, and flow rates are ideally distributed within a system rather than the results of friction-based flow distribution. This makes it difficult to model, test and verify actual control. Third, different numerical solvers for differential equations might be needed for different use cases [10]. However, most traditional tools have predefined solvers in their physical component models. Forth, these tools are hard to support fast prototyping based on various user's needs. For example, the control logic for the WSE in DOE2.2 are predefined. Users are able to change the thresholds of particular conditions, but not the logic themselves. It is difficult for users to implement new logic. Fifth, these tools are difficult to perform multi-domain simulations. For example, to study the interactive performance of the thermal and the electrical system, one needs an external data synchronizer to couple these tools with electrical simulation tools as mentioned in Ref. [11].

Equation-based languages such as Modelica [12] can provide solutions to the above-mentioned issues. Modelica separates physical equations and numerical solvers wherever possible. The separation can mitigate the risks of intertwinement, and can fully take advantages of different expertise from different domains. For example, model developers can concentrate on how to develop efficient high-fidelity physical models, while computer engineers can focus on the development of robust numerical solvers. Also, the State Graph package [13] in the Modelica Standard Library can be used to perform discrete control which contains dead band or delay time. The rich library of numerical solvers in Modelica can be chosen for different systems and different use cases. Besides, Modelica models are convenient enough to be extended to support fast modeling and simulation. Furthermore, Modelica itself supports multi-domain simulation. Models from different domains are built in one single platform so that dedicated data synchronizer between different platforms is not required.

The Modelica Buildings library is designed to model and simulate the energy and control system at building and community level [14]. The Buildings library is free open-source, and has been demonstrated to have full capability to conduct energy efficiency analysis. Researchers have been active to utilize the Buildings library in a broad range of applications, such as dynamic modeling [15]–[18], rapid prototyping of a district heating system [19], evaluation of feedback control [8], fault detection and diagnosis at the whole building level [20], optimal model-based control design and evaluation [21], [22], as well as coupled simulation between the cooling system and the detailed room model with fluid dynamics considered [23], [24].

This study creates a new data center package using the equation-based modeling language Modelica and releases the package in the open source Modelica Buildings library to support fast

modeling and simulation of cooling systems for data center applications. Those new models are able to predict thermal, mechanical and electrical dynamics of conventional and renewable data centers. As some of the data center cooling systems, such as chiller plants, are also commonly used by large commercial buildings and district cooling systems, the models developed by this study can also be used for those applications. This paper first introduces typical air-cooled cooling systems in data centers such as chilled water system and direct expansion (DX) system. In Section 3, we give an introduction of the component models, subsystem models, cooling control models, and system models in the data center package. In Section 4 and 5, to demonstrate the capability of Modelica-based tools, we model and simulate a cooling system under normal operation and emergency operation for a conventional and renewable data center respectively. We then conclude the paper in Section 6.

2 Air-cooled Cooling Systems

Many different cooling systems have been designed and operated for data centers. The data center room can be cooled by air, single- or two-phase liquid at room, rack or even chip level. However, the majority of existing data centers are cooled by air [25]. Thus, our current modeling efforts focus on air-cooled systems. The air-cooled systems supply to the data center room cold air, which is then drawn by the rack or servers [26]. The air can be cooled by chilled water systems or DX systems, which are introduced next.

2.1 Chilled Water Systems

Chilled water systems are usually used for large data centers. A typical chilled water system includes chillers, Computer Room Air Handlers (CRAHs), pumps, and cooling towers, as shown

in Figure 1(a). The heat generated in the data center room is first transferred to the chilled water through the CRAHs, and the chillers then transfer the heat from the chilled water loop into the condenser water loop through a refrigeration system. The cooling towers at last reject the heat in the condenser water loop to the outdoor environment.

Economizers can also be installed to provide auxiliary cooling when outdoor conditions allow. The economizer can be installed on either the air side (e.g. ASE) or the water side of chilled water system (e.g. WSE). WSE can be configured with a chiller in different ways [9]. For example, the WSE can be integrated with the chiller, meaning that the economizer can meet all or some of the load while the chiller meets the rest of the load, or non-integrated, meaning the economizer can only operate when it can meet the entire load.

A common configuration of a chiller plant with integrated WSE is shown in Figure 1(b). The WSE is located upstream of the chiller on the load side of the common leg. This configuration can guarantee that the WSE can meet the warmest return chilled water and maximize the number of hours when WSE can operate. The chiller plant with integrated WSEs can operate in three modes: Free Cooling (FC) mode when only the WSE is enabled for cooling, Partial Mechanical Cooling (PMC) mode when the chiller and WSE are both triggered, and Full Mechanical Cooling (FMC) mode when only the chiller is activated. When a particular cooling mode should be activated is determined by a cooling mode controller, as described in Section 3.3.1, and how to achieve the cooling mode is determined by the manipulation of the associated isolation valves V_1 to V_4, the chiller bypass valve (V_6) and the WSE bypass valve (V_5), as shown in Section 3.3.3.

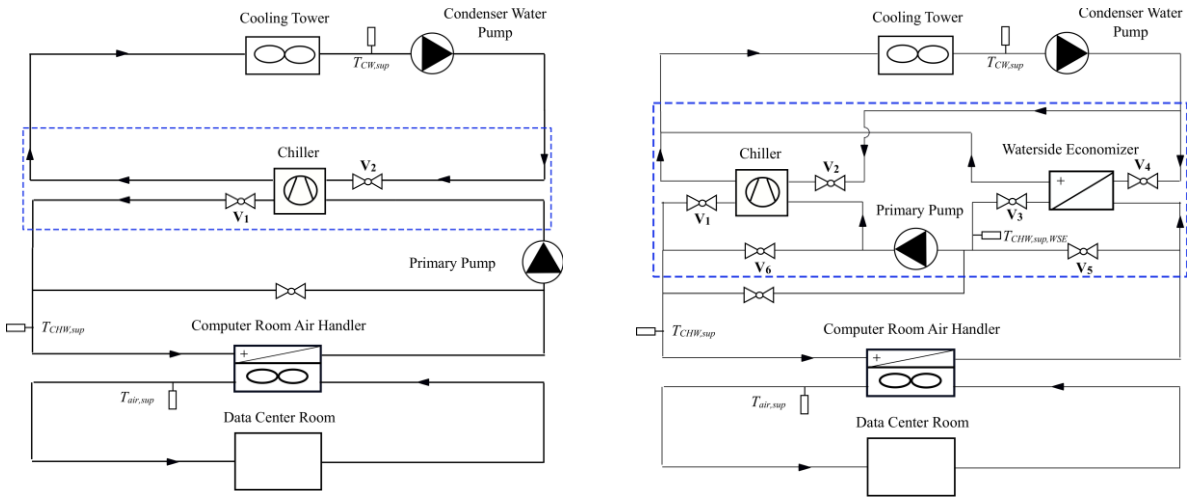

(a) Without WSE (b) With an integrated WSE on the load side

Figure 1. Primary-only chilled water system

2.2 DX Systems

DX systems are widely used in small data centers as a primary cooling system or as a backup system for the chilled water system. The major cooling source in a DX system are the Computer Room Air-Conditioner (CRAC) units. CRAC units typically have their own refrigeration system. They absorb heat from the data center room through evaporators, and reject heat to the outdoor environment (air-cooled CRAC) or a condenser water loop (water-cooled CRAC) through condensers. Based on the type of the condenser in the CRAC, the DX system is categorized into two classes: air-cooled or water-cooled. Figure 2(a) shows a schematic drawing for an air-cooled DX system, where the air-cooled CRAC is installed to cool the return air and send it back to the data center room by supply air fans. The heat extracted by the CRAC is then rejected to the outdoor environment through condenser fans. The DX system is usually installed together with ASEs, for example, as shown in Figure 2(b). The ASEs enable the system to efficiently use the cold outdoor

air and reduce the operating time of CRACs.

In Figure 2(b), with an ASE, the air-cooled DX system can also operate in the three modes mentioned in Section 2.1. The only difference is that the mechanical cooling is provided by the CRACs in the air-cooled DX system instead of the chillers as in the chilled water system. Similarly, when to activate a particular cooling mode is determined by the cooling mode controller, and how to achieve the cooling mode is determined by the manipulation of the dampers such as D_1 to D_4 in Figure 2(b) [9].

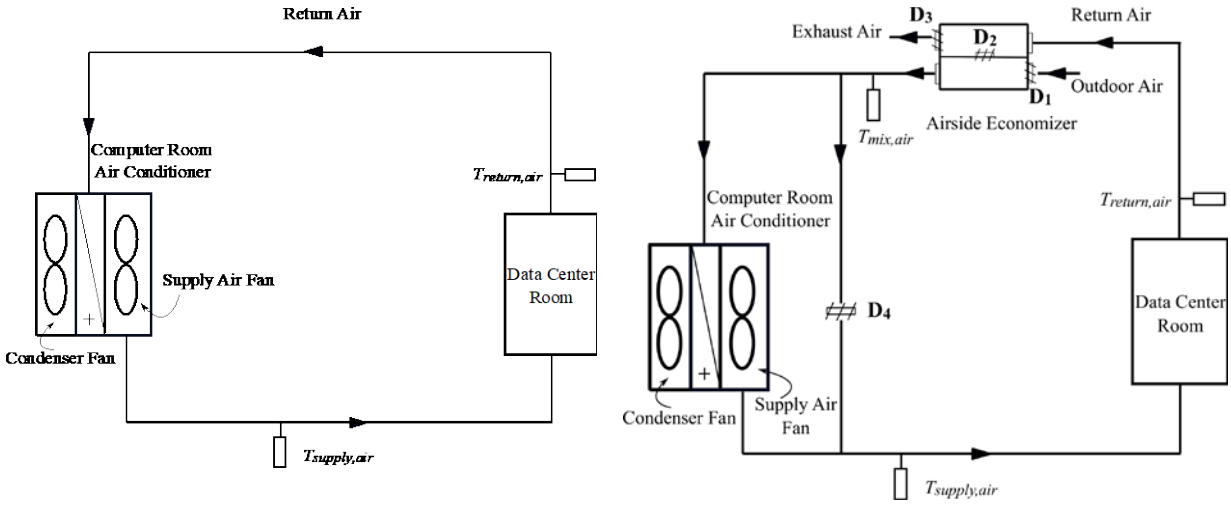

(a) Without ASE (b) With an ASE

Figure 2. Air-cooled DX system

3 Model Implementation

The data center package *Buildings.Applications.DataCenters* is built on Modelica Buildings library and Modelica Standard library as shown in Figure 3, and was publicly released in the Modelica Buildings library 5.0.0 (https://simulationresearch.lbl.gov/modelica/). It contains

component models for the abovementioned two typical air-cooled cooling systems in data centers. This package adopts the class hierarchy used by the Buildings library, and contains various reusable base classes. These base classes together with the inheritance and instantiation in the object-oriented modeling language Modelica facilitate fast model-based design of data center cooling systems. The following part introduces some of the key models for cooling components, subsystems, controls and system templates.

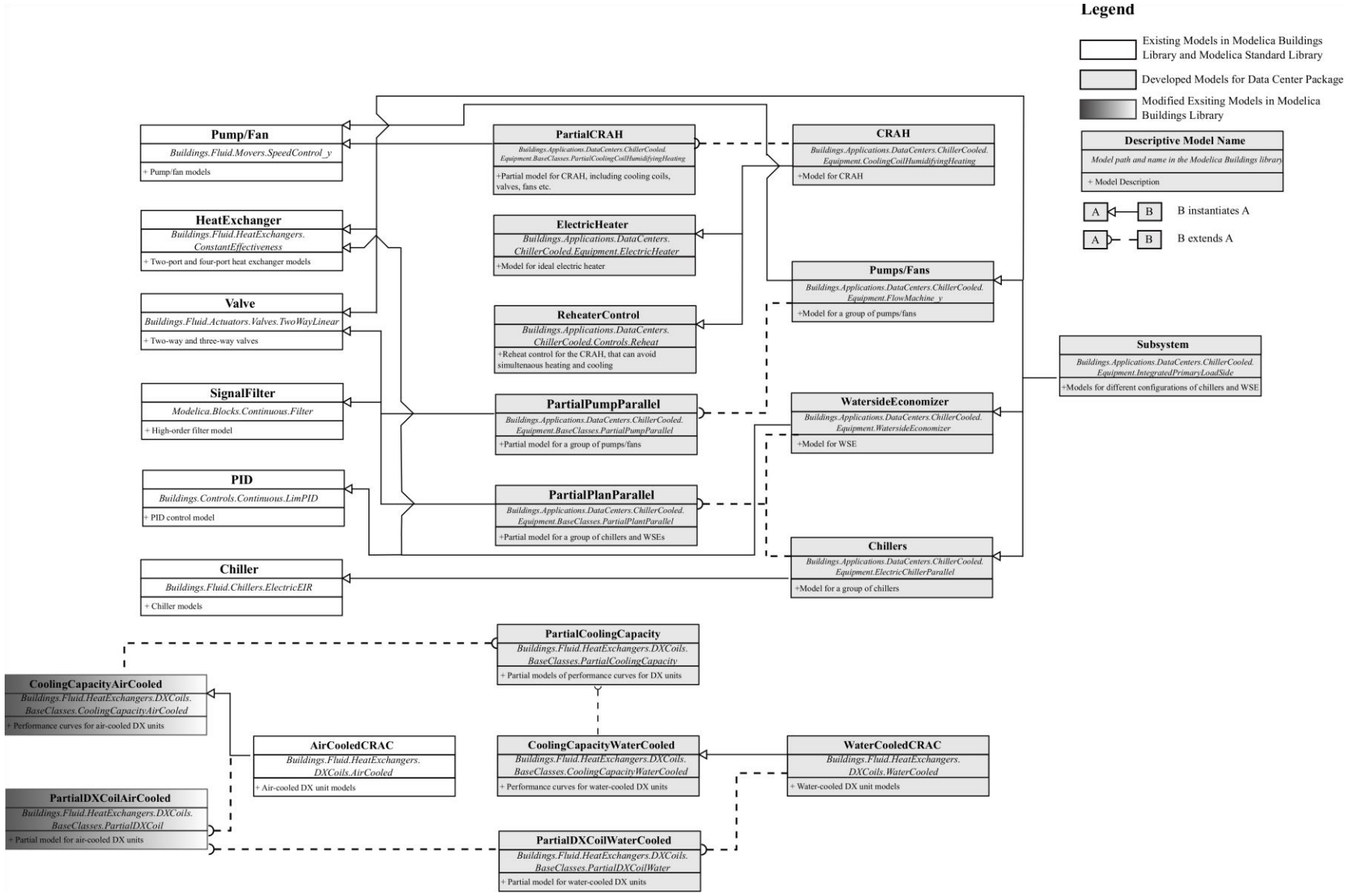

Figure 3. Class inheritance and instance diagram for part of the data center package

3.1 Cooling Component Models

3.1.1 Group of Equipment

A group of chillers and pumps can be modeled on the base of existing chiller and pump model respectively. Take as an example the model of a parallel of chillers. The diagram for the ready-to-use model for the chiller parallel is shown in Figure 4. This model utilizes existing chiller and valve models in Modelica Buildings library and a filter model in Modelica Standard library.

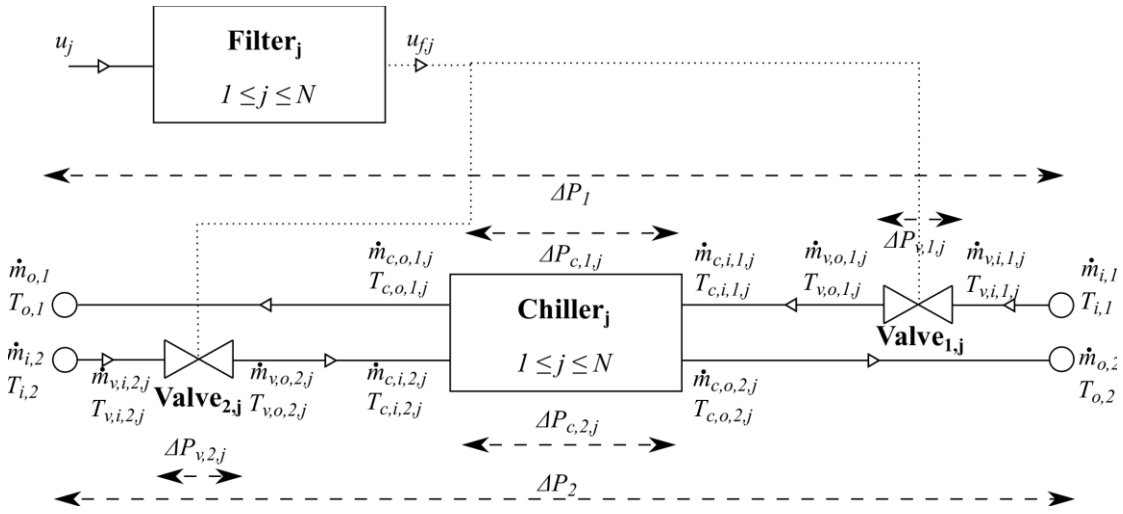

Figure 4. Diagram of the new chiller parallel model

$$\left(T_{c,o,k,j}, \dot{m}_{c,o,k,j}, \Delta P_{c,k,j}\right) = chiller\left(T_{c,i,k,j}, \dot{m}_{c,i,k,j}, u_j\right), \tag{3}$$

$$\left(T_{v,o,k,j}, \dot{m}_{v,o,k,j}, \Delta P_{v,k,j}\right) = valve\left(T_{v,i,k,j}, \dot{m}_{v,i,k,j}, u_{f,j}\right), \tag{4}$$

$$u_{f,j} = filter\left(u_j\right). \tag{5}$$

In the above equations, T, $\dot{m}$, and ΔP are temperature, mass flow rate and pressure losses respectively. For the subscripts, c, v and f are short for chiller, valve and filter, i and o refer to the inlet and the outlet, k represents the two sides of the equipment with 1 denoting evaporator side and 2 denoting condenser side, and j is the index of equipment ranging from 0 to N, where

N is the design number of the chiller in the group. The functions $chiller, valve,$ and $filter$ represent existing chiller, valve and filter model, respectively. The chiller model can be referred to [27], and the valve model can be referred to [28]. For the filter model, we use a second-order critical damping low pass filter to smooth the input control signal in order to represent the mechanical inertia in the equipment such as valves as introduced in [14]. Detailed equations are shown in Eq.(6)~(8). a is the coefficient of the state space equations for the first-order filter described in Eq.(7) and (8). f_{cut} is the cut-off frequency of the low pass filter, which passes signals with a frequency lower than f_{cut} and attenuates signals with a higher frequency. α is a frequency correction factor for different orders. Here we use 0.622 for the second order. u is the input signal, and u_f is the output signal from the filter.

$$a = -\frac{2\pi f_{cut}}{\alpha}, \tag{6}$$

$$\frac{dx}{dt} = a(x - u), \tag{7}$$

$$\frac{du_f}{dt} = a\left(u_f - x\right). \tag{8}$$

The group model is built by connecting the abovementioned individual component together in a way that the chillers are in parallel with each other, one valve is at the upstream of each side of each chiller, and each valve receives the signal of position from the filters. The mass flow rate at each component on each side such as $\dot{m}_{v,i,k,j}$ is calculated based on the pressure balance in the fluid network by combining Eq.(3) through Eq.(13). $\dot{m}_{i,k}$ and $T_{i,k}$ are the mass flow rate and temperature at the inlet of the group.

$$\dot{m}_{i,k} = \sum_{j=1}^{N} \dot{m}_{v,i,k,j}, \tag{9}$$

$$\dot{m}_{c,i,k,j} = \dot{m}_{v,o,k,j}, \tag{10}$$

$$T_{i,k} = T_{v,i,k,j}, \tag{11}$$

$$T_{c,i,k,j} = T_{v,o,k,j}, \tag{12}$$

$$\Delta P_{c,k,1} + \Delta P_{v,k,1} = \cdots = \Delta P_{c,k,j} + \Delta P_{v,k,j}. \tag{13}$$

The outlet conditions of the grouped chillers such as mass flow rate $\dot{m}_{o,k}$, temperature $T_{o,k}$ and pressure loss ΔP_k are then obtained as follows:

$$\dot{m}_{o,k} = \sum_{j=1}^{N} \dot{m}_{c,o,k,j}, \tag{14}$$

$$\dot{m}_{o,k} T_{o,k} = \sum_{j=0}^{N} \dot{m}_{c,o,k,j} T_{c,o,k,j}, \tag{15}$$

$$\frac{1}{\Delta P_k} = \sum_{j=1}^{N} \frac{1}{\Delta P_{c,k,j} + \Delta P_{v,k,j}}. \tag{16}$$

The implementation of the grouped chillers in Modelica benefits from the data structure *array*, which can vectorize the existing chiller model directly. The vectorized equipment model uses the same design parameters, but different performance curves if needed. The pseudo-code of vectorized chiller model *ElectricChillerParallel* is shown in Figure 5(a). First, a partial class of the electric chiller model *Fluid.Chillers.BaseClasses.PartialElectric* is instantiated through vectorization with a number n, which specifies the length of the chiller array. The keyword *replaceable* allows the model to be redeclared with a detailed chiller model later on. Line 3 specifies the medium used in the chillers. Line 4 defines the identical design parameters for the chillers with the keyword *each* in Modelica, such as the design capacity. Line 5 defines the performance curves of each chiller by assigning different curves from a performance curve array. The same instantiation method is also used to model a group of pumps. In addition, we add

isolation valves in the vectorized models to avoid circulating flow among components. The implemented source code is packaged in a model and the graphic icon shown in Figure 5(b) is added to support graphical modeling.

```
1: replaceable Fluid.Chillers.BaseClasses.PartialElectric chillers[n]
2: constrainedby Fluid.Chillers.BaseClasses.PartialElectric(
3:       redeclare each final replaceable package Medium = Medium,
4:       each final parameters = parameters,
5:       final performanceCurve = performanceCurveArray)
6: "Chillers with identical design parameters but different performance curves"
```

(a) Pseduo code

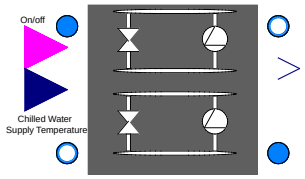

(b) Modelica icon

Figure 5. Vectorized chiller model in Modelica

3.1.2 Waterside Economizer

The WSE model is built using a heat exchanger model with constant effectiveness, and a three-way valve model. The mathematical equations that define the distribution of fluid flow is similar to that in Section 3.1.1. Figure 6 shows the Modelica implementation. The three-way valve is on the chilled water side, and can be adjusted to control the chilled water supply temperature using a built-in PI controller. The three-way valve can be activated or deactivated based on users' needs for different control strategies. For example, in the FC mode, the mechanical cooling is shut down, and only the WSE is activated to provide cooling. The chilled water supply temperature downstream of the WSE can be controlled at its set point by regulating the speed of the cooling tower fans or by modulating the three-way valve on the chilled water side in the WSE. The former control strategy requires deactivation of the three-valve, while the latter control needs to activate the three-way valve. The switch between activation and deactivation of the three-way valve is

realized by setting a Boolean parameter *activateControl* to *True* or *False*.

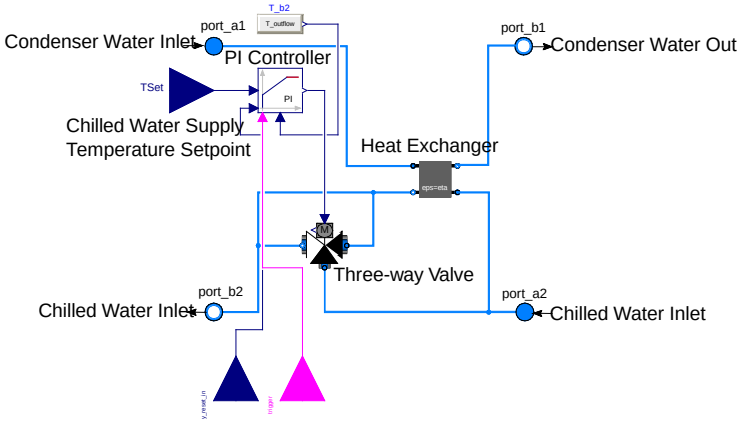

Figure 6. Waterside economizer model in Modelica

3.1.3 Computer Room Air Handler

As shown in Figure 7(a), the CRAH model named *CoolingCoilHumidifyingHeating* is built on the existing models of a cooling coil, a humidifier, a fan and a two-way valve on the water side of the cooling coil. An ideal electric reheater and an on/off controller with hysteresis is added in order to avoid simultaneous heating and cooling.

The electrical reheater is modeled as an ideal heat transfer process. The required heat flow $\dot{Q}_r$ to control the outlet temperature at its setpoint $T_{a,s}$ is shown in Eq.(17). And the power of the electrical heater P is then obtained in Eq.(18).

$$\dot{Q}_r = \max\left(0, \dot{m}_a C_{p,a}\left(T_{a,s} - T_{a,i}\right)\right), \tag{17}$$

$$P = \eta \dot{Q}_r. \tag{18}$$

The electrical reheater is activated only if the following two conditions are met simultaneously:

$$y_{w,v} \leq y_{w,v,sh} - \Delta y \tag{19}$$

$$T_{a,o} - T_{a,s} \leq dT_{sh} - \Delta \mathrm{d}T \tag{20}$$

where $y_{w,v}$ is the two-way valve position, $y_{w,v,sh}$ is a user-defined switching threshold, $T_{a,o}$ is the outlet air temperature, $T_{a,s}$ is the outlet air temperature setpoint, dT_{sh} is a user-defined temperature difference threshold, Δy and $\Delta \mathrm{d}T$ are the control dead band for the valve position and temperature difference. These two conditions mean that the electric reheater is only activated when the valve on the waterside reaches its minimum position, and the outlet temperature is still lower than its setpoint.

3.1.4 Computer Room Air Conditioner

Both air-cooled and water-cooled CRAC models are available in Modelica Buildings library. The capacity of the refrigeration system in the CRAC is expressed using regression equations based on inlet temperature and flowrate on both the evaporator and condenser sides. The water-cooled CRAC model in Modelica is shown in Figure 7(b), and detailed equations are illustrated as below.

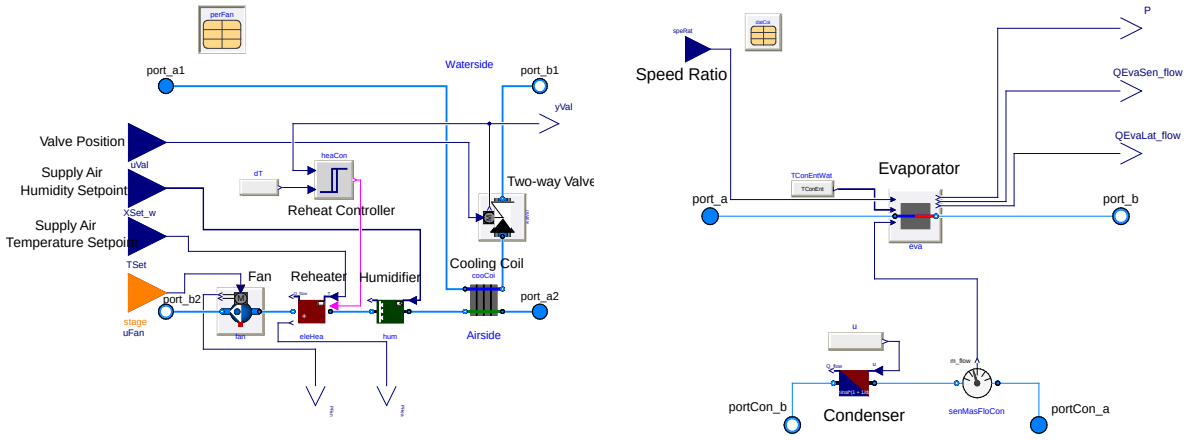

(a) CRAH model (b) CRAC model

Figure 7. Modelica Implementation of CRAH and CRAC models

This model uses the coil bypass factor (*bf*) to calculate sensible and latent heat thorough the cooling coils. The coil bypass factor at nominal conditions bf_0 can be calculated as:

$$bf_0 = \frac{h_{a,o,0} - h_{ADP,0}}{h_{a,i,0} - h_{ADP,0}}, \tag{21}$$

where $h_{a,o}$ and $h_{a,i}$ are the enthalpy of air at the outlet and inlet respectively, h_{ADP} is the enthalpy of saturated air at the coil apparatus dew point, and subscript 0 is the nominal condition.

The model uses modifiers to correct the nominal values in order to predict the off-design conditions. For example, Eq.(22) and (23) show the calculation of the available total cooling capacity $\dot{Q}_{t,a}$ and energy input ratio EIR from their corresponding nominal values ($\dot{Q}_{t,a,0}$ and EIR_0) and the modifiers (g_1 to g_6). r_a and r_w are air and water flow ratio as defined in Eq.(24) and (25), g_1 and g_4 are biquadratic equations, and g_2, g_3, g_5, g_6 are polynomial equations. These modifier equations can be obtained from curve-fitting techniques.

$$\dot{Q}_{t,a} = \dot{Q}_{t,a,0} g_1\left(T_{a,wb,i}, T_{w,i}\right) g_2(r_a) g_3(r_w), \tag{22}$$

$$EIR = EIR_0 g_4\left(T_{a,wb,i}, T_{w,i}\right) g_5(r_a) g_6(r_w), \tag{23}$$

$$r_a = \frac{\dot{m}_a}{\dot{m}_{a,0}}, \tag{24}$$

$$r_w = \frac{\dot{m}_w}{\dot{m}_{w,0}}. \tag{25}$$

The sensible heat ratio (SHR) in the cooling coil is calculated using Eq.(26), where $h_{T_{a,i},w_{ADP}}$ is the enthalpy of the fictitious air with the same dry bulb temperature of the actual inlet air $T_{a,i}$ and the same humidity ratio of the saturated air at coil apparatus dew point condition w_{ADP}, $h_{a,i}$ is the enthalpy of the actual inlet air, and h_{ADP} can be calculated from Eq.(27).

$$SHR = \frac{h_{T_{a,i},w_{ADP}} - h_{ADP}}{h_{a,i} - h_{ADP}}, \tag{26}$$

$$h_{ADP} = h_{a,i} - \frac{\dot{Q}_{t,a}}{\dot{m}_a(1 - bf)}. \tag{27}$$

The power consumption by the compressor P and heat rejection in the water-cooled condenser $Q_{t,w}$ can be calculated as

$$P = \dot{Q}_{t,a} EIR, \tag{28}$$

$$\dot{Q}_{t,w} = \dot{Q}_{t,a}(1 + EIR). \tag{29}$$

The outlet conditions on the air side are then calculated based on $\dot{Q}_{t,a}$ and SHR as shown in following equations:

$$m_a \frac{dh_{a,o}}{dt} = \dot{m}_a\left(h_{a,i} - h_{a,o}\right) - \dot{Q}_{t,a}, \tag{30}$$

$$m_a \frac{dw_{a,o}}{dt} = \dot{m}_a\left(w_{a,i} - w_{a,o}\right) - \frac{(1-SHR)\dot{Q}_{t,a}}{h_{g,w}}. \tag{31}$$

In the above two equations, $h_{g,w}$ is the latent heat of condensation of water, whose value is 2442

J/g at 25℃, and m_a is the mass of the air volume in the evaporator. Here assuming that the density of the air keeps constant, we can get

$$m_a = \tau_{a,0}\dot{m}_{a,0}, \tag{32}$$

where $\tau_{a,0}$ is the design thermal time constant of the evaporator, and can be defined by users.

The outlet temperature of the water-cooled condenser $T_{w,o}$ can then be obtained from Eq.(33). $C_{p,w}$ is the specific heat capacity of water, and m_w is the mass of the water volume of the condenser, that also can be calculated from user-defined time constant $\tau_{w,0}$ as shown in Eq.(34).

$$m_w C_{p,w} \frac{dT_{w,o}}{dt} = \dot{m}_w C_{p,w}\left(T_{w,i} - T_{w,o}\right) - \dot{Q}_{t,w}, \tag{33}$$

$$m_w = \tau_{w,0}\dot{m}_{w,0}. \tag{34}$$

3.2 Subsystem Models

Different subsystem models and their base classes that define the arrangement of chillers and WSE are also built. The different subsystem models share the same base class as shown in Figure 8(a). The base class is built on a four-port fluid interface, representing the inlets and outlets for the chilled and condenser water, with instances of the chiller group model and the WSE group model. The connections of chillers and WSE on the chilled water side are not declared in the base class, because different subsystem models mentioned in Ref. [9] have different hydraulic configurations, such as chillers with integrated WSE on the load side, chillers with integrated WSE on the plant side, and chillers with nonintegrated WSE etc..

The different subsystems can then be modelled individually using a hierarchical approach. In this case, we first inherit the base class, then instantiate additional necessary equipment models, and

finally add physical connections among components. For example, to model the subsystem where the WSE is integrated on the load side of a primary-only chilled water system (as shown in the dashed box of Figure 1(b)), we only need to extend the base class, add necessary instances such as bypass valves and pumps, expose model inputs and outputs, and finally connect them as in an actual system. Figure 8(b) shows the implementation of such a subsystem model based on the base class in Figure 8(a). On the left are the model inputs, including the on/off command, supply chilled water temperature setpoint, bypass valve position signal and pump speed signal from particular controllers. On the right are the model outputs, such as power from chillers and pumps.

This hierarchical modeling structure allows users to manage the complexity of large models, and to assemble system models as one would connect components in an actual system. This structure also facilitates debugging and verification of component models. For example, a lower-level model is first debugged and verified, and then instantiated in a higher-level model, which can help identify modelling errors at the early stage of the model development.

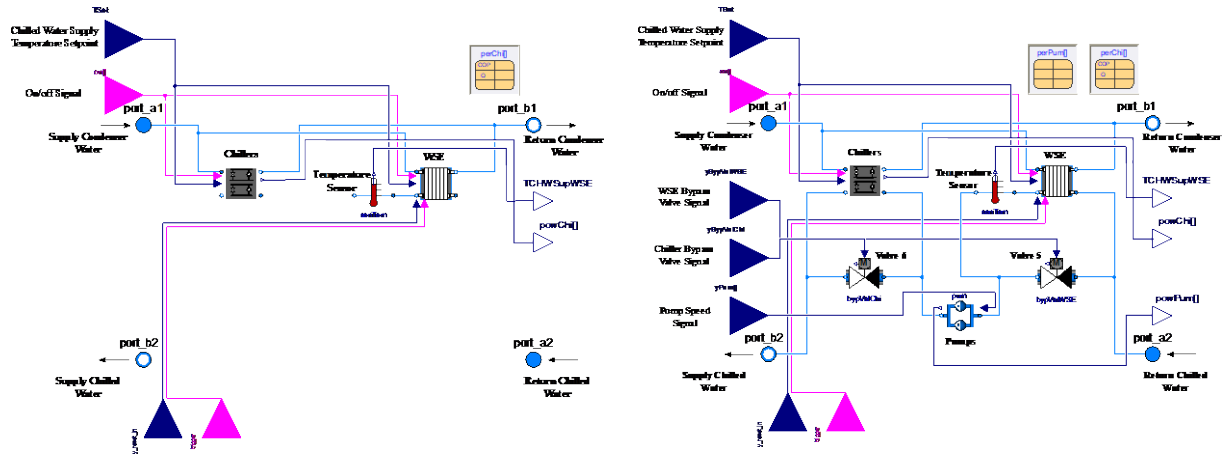

(a) Base class (b) Integrated WSE on the load side

Figure 8. Modelica implementation of chillers and WSE subsystem

3.3 Control Models

3.3.1 Cooling Mode Control

As described in Section 2, in both the chilled water and DX systems, a cooling mode control determines when to activate and deactivate the FC, PMC and FMC modes for the cooling system with economizers based on the system status and the environment. The cooling mode control is a supervisory control, and the output control signal will be taken as inputs by other equipment-level controllers as described in Section 3.3.2.

The cooling mode can be described as a finite-state machine. The cooling mode can transition from one state to another in response to some external inputs. For example, we can present a widely-used control strategy [29] for a chilled water system with integrated WSE using a state graph as shown in Figure 9(a). The chiller is switched on when

$$\Delta t_{c,off} \geq \Delta t_1 \quad and \quad T_{chw,sup,wse} > T_{chw,sup,set} + \Delta T_1 \ \ for \quad \Delta t_2, \tag{35}$$

and it is switched off when

$$\Delta t_{c,on} \geq \Delta t_3 \quad and \quad T_{chw,sup,wse} < T_{chw,sup,set} - \Delta T_2 \ \ for \quad \Delta t_4, \tag{36}$$

where $\Delta t_{c,off}$ is the time of the chiller in Off status, $\Delta t_{c,on}$ is the elapsed time since the chiller was switched on, Δt_1 to Δt_4 are time thresholds whose defaulted values are shown in Figure 9(a), $T_{chw,sup,wse}$ is the temperature of the supply chilled water downstream of the WSE, $T_{chw,sup,set}$ is the chilled water supply temperature set point, and ΔT_1 and ΔT_2 are the dead band temperature. The waiting time and dead band can prevent frequent short cycling.

The WSE is enabled when

$$\Delta t_{wse,off} \geq \Delta t_7 \quad \text{and} \quad T_{chw,ret,wse} > T_{wb} + T_{app,ct,pre} + \Delta T_4 \quad for \quad \Delta t_8, \tag{37}$$

and it is disabled when

$$\Delta t_{wse,on} \leq \Delta t_5 \quad \text{and} \quad T_{chw,ret,wse} < T_{chw,sup,wse} + \Delta T_3 \quad for \quad \Delta t_6, \tag{38}$$

where $\Delta t_{wse,off}$ is the elapsed time of the WSE in Off status, $\Delta t_{wse,on}$ is the elapsed time since the WSE was switched on, $T_{chw,ret,wse}$ is the temperature of the return chilled water upstream of the WSE, T_{wb} is wet bulb temperature of the outdoor air, $T_{app,ct,pre}$ is the predicted approach temperature of the cooling tower, ΔT_3 and ΔT_4 are the offset temperature, and Δt_5 to Δt_8 are time thresholds. In our application, we set $T_{app,ct,pre}$ as the nominal approach temperature in the cooling tower, although many other prediction algorithms can be used such as using a detailed cooling tower model [29] or engineering experience [30]. Figure 9(b) shows the Modelica implementation using the State Graph package.

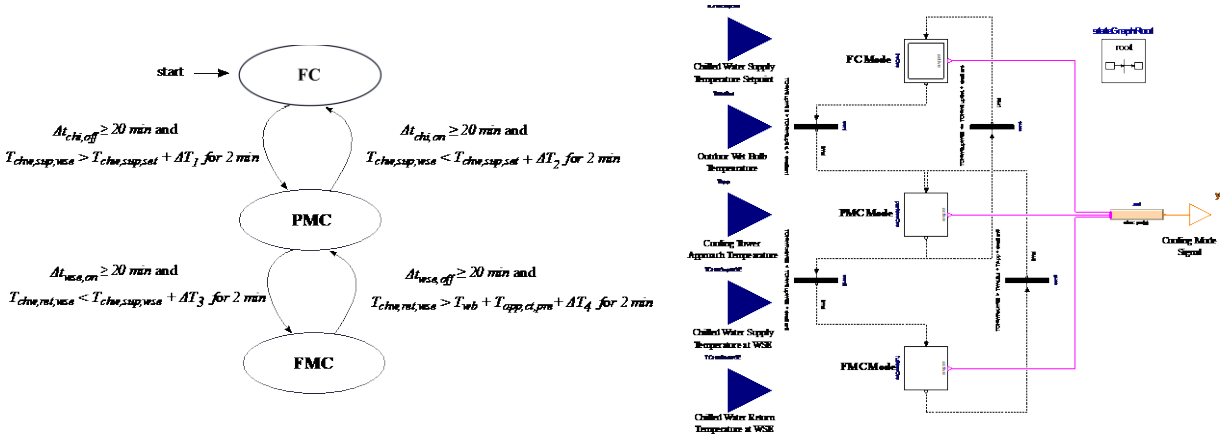

(a) State graph (b) Modelica implementation

Figure 9. Cooling mode control for a chilled water system with integrated WSEs

3.3.2 Equipment Control

Equipment-level control includes stage control and speed control of chillers, pumps and cooling towers. The stage control determines when and how many equipment are activated at a given time. The speed control regulates the speed of equipment such as cooling tower fans.

For the stage control of chillers, we adopted the following logic: If the cooling mode control outputs FC mode, then all chillers are commanded off. If the cooling mode control outputs PMC or FMC mode, at least one chiller should be active all the time. One additional chiller is commanded on when

$$\dot{Q}_{ave} > \dot{Q}_{up} + \Delta \dot{Q} \quad \text{for} \quad \Delta t_9, \tag{39}$$

and commanded off when

$$\dot{Q}_{ave} < \dot{Q}_{down} - \Delta \dot{Q} \quad \text{for} \quad \Delta t_{10}, \tag{40}$$

where $\dot{Q}_{ave}$ is the average cooling load in all the active chillers at the current time, $\dot{Q}_{up}$ and $\dot{Q}_{down}$ are the cooling load thresholds for staging up and down, respectively, and $\Delta \dot{Q}$ is a deadband. The two conditions need to remain true for a predefined waiting time Δt_9 and Δt_{10}, respectively. The stage control was implemented in Modelica using the State Graph package.

For the speed control, here we take the cooling tower fans as an example. The cooling tower fan speed should be regulated differently in different cooling modes. One possible set of control logics is shown as follows.

- In the FC mode, the fan speed is controlled to maintain a predefined chilled water supply

temperature downstream of the WSE.

- In the PMC mode, the fan speed is reset to 90%. Setting the speed to 100% can produce the condenser water as cold as possible and maximize the WSE output. However, with variable speed drives on the tower fans, changes from 90% to 100% do little to lower the condenser water temperature but increases the fan energy significantly [29].
- In the FMC mode, the fan speed is controlled to maintain the supply condenser water at its set point.

3.3.3 Valve Control

The transition among each cooling mode is achieved by manipulating the associated isolation valves and bypass valves. For example, in Figure 1(b), when the cooling system is in the FC mode, the isolation valves V_1 and V_2 in chillers, and V_5 for bypassing the WSE are shut off. The isolation valves V_3 and V_4 in the WSE, and V_6 for bypassing the chillers are fully opened so that the chilled water can flow through the WSE, and then be delivered by the primary pumps to the CRAHs. In the PMC mode, V_1 and V_4 are fully open, and V_5 and V_6 are closed. In the FMC mode, while V_3, V_4 and V_6 are closed, V_1, V_2 and V_5 are fully open to deliver the chilled water through the primary pumps, chillers, and then CRAHs.

3.4 System Templates

Templates for different systems are also provided. An example is shown in Figure 10, where the model of a primary-only chilled water system with an integrated WSE, its control system, boundary conditions, and post-processor is presented.

The boundary conditions for the cooling system are read from a weather data file. The cooling and control system are assembled by connecting the above-mentioned component and control models.

The data center room model in the cooling system is simplified using a well-mixed volume, because the air flow management in the room is not the focus here. The cooling load is assumed to be constant during the simulation period. Post-processing provides an option to process the simulation results such as energy and control performances in the model. The simulation results of the system template model have been reported in Ref. [9].

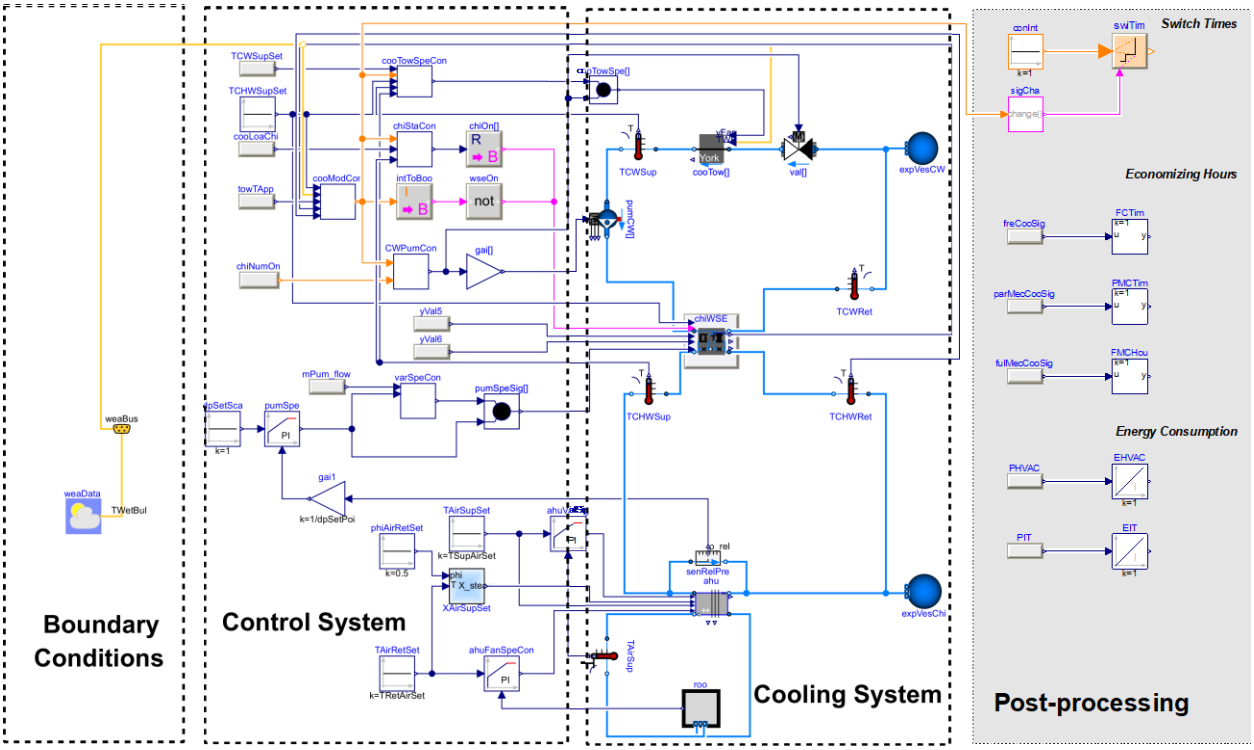

Figure 10. Modelica implementation of a primary-only chilled water system with an integrated WSE

3.5 Model Evaluation

Each component is verified in a simulation example, following the conventions of the Buildings library [14]. Taking advantages of the class hierarchy in the Buildings library and the object-oriented language Modelica, we built the data center package based on the base classes and ready-

to-use component models. We validated the data center package using analytical verification and comparative testing. The former has also been used to validate all individual component models in the Buildings library. For example, the WSE model is validated by analytical verification, which compares its results with analytical solutions that are derived for certain steady-state boundary conditions. In addition, the CRAC model in Modelica is validated by comparing its simulation results with the same model in EnergyPlus.

4 Case Study 1: Conventional Data Center Operation

This case study presents two scenarios to investigate the cooling system operation in a conventional data center located in Salem, Oregon, USA. This data center is powered by the power grid. The first scenario investigates the energy efficiency and control performance of the cooling system under normal operation (e.g. connected to grid), and the other one compares different operation strategies to explore the opportunities of effective operation of the cooling system under emergency situations (e.g. disconnected from grid and backup generators).

4.1 Description of Cooling and Electrical System

Data centers are required to operate 24 hours per day, 365 days per year. Electrical distribution systems in data centers are designed to power the IT equipment in a safe and reliable manner. One typical design is to power the data center with multiple sources. For example, data centers normally draw three-phase AC power from the power grid, and use diesel generators as backups during power grid failures. There is usually a time gap between the power grid failure and the activation of the backup diesel generators, because the diesel generators usually need a short warmup time. To guarantee the safety of the data center during this time gap, the energy storage system, the so-called Uninterruptible Power System (UPS), is utilized to provide power. The UPS is typically

sized to guarantee a 15-minute emergency power delivery for IT equipment of a fully-loaded data center and the critical equipment in the cooling system. The emergency operation of the UPS ends once the backup generators are brought online or the power grid recovers. The schematic drawing of a typical data center cooling and electrical system is shown in Figure 11. The fluid flow in the cooling system is denoted by solid lines, and the power flow in the electrical system is denoted by dashed lines.

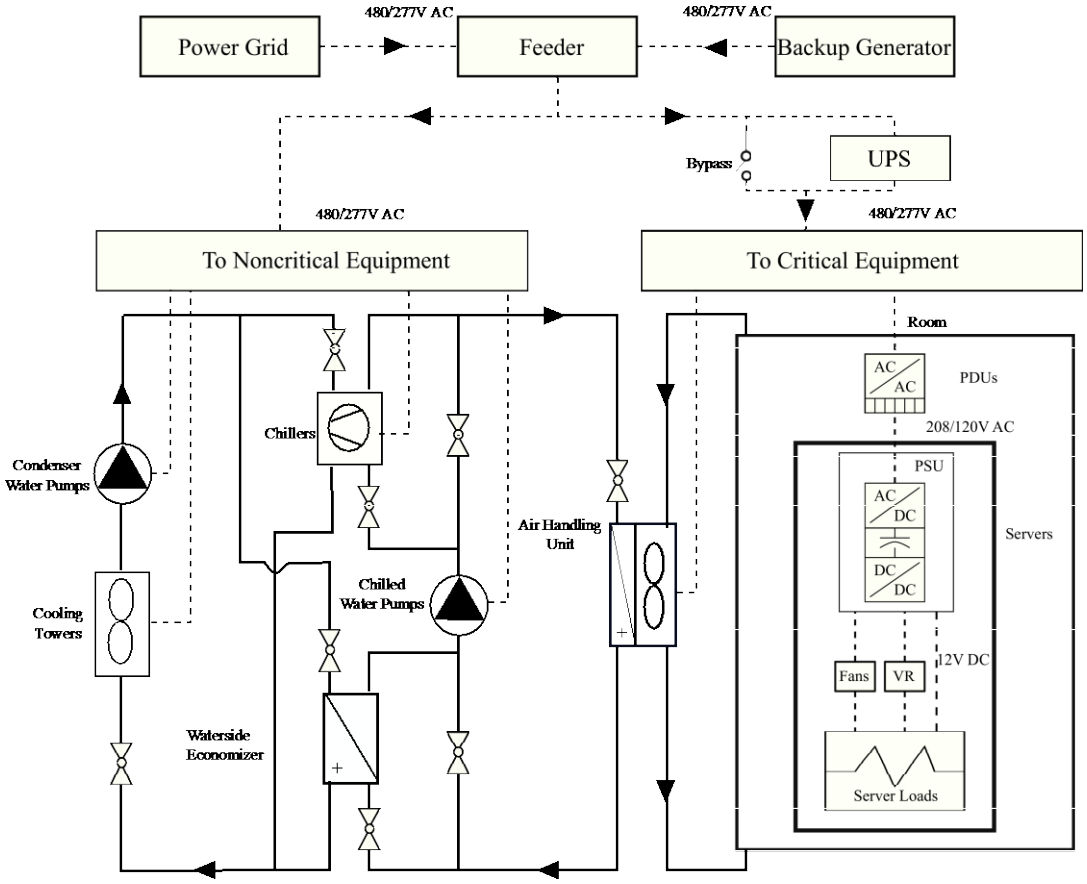

Figure 11. Schematic drawing of the cooling and electrical system in a data center

4.1.1 Cooling System

In the case study, the studied data center is cooled by a primary-only chilled water system with

two identical chillers and one integrated WSE on the load side. The WSE is installed in parallel with chillers on the condenser water side. The design cooling load is 2,200 kW, which could be satisfied by two identical chillers in the FMC mode or one WSE in the FC mode. The number of variable-speed chilled water pumps, constant-speed condenser water pumps and variable-speed cooling towers are equal to the number of chillers. One CRAH with one supply air fan delivers cold air to the room. The evaluation of the redundancy for the cooling system, such as a backup CRAH and redundant piping system, is not a purpose of this case study, therefore it is not considered here.

Dynamics in the cooling system models are represented using two methods: one is a lumped volume, parameterized by time constant or thermal mass, and the other is a signal filter that filters high frequency input signals. For example, the dynamics in the cooling coils are represented by a predefined time constant of 30s, and the thermal mass of the racks and the servers from Ref. [31] are added to the data center room model to calculate the thermal inertia inside the data center room. Furthermore, the dynamic behavior of the valve's motors is represented by adding a second-order filter for the input position signals. For the control system, the room temperature is controlled at a set point of 25 °C by adjusting the fan speed in the CRAH. The supply air temperature is maintained at 18 °C by regulating the two-way valve on the waterside of the cooling coils. The chilled water supply temperature is set to be 6.5 °C under all cooling modes and load conditions.

4.1.2 Electrical System

The configuration of a power distribution system for the data center in North America is represented by the one-line diagram in Figure 11 [32]. Note that in real data centers the electrical architecture has much more complexity and diversity. Based on their importance to keep the data center uninterrupted, all the equipment including IT and cooling equipment in a data center can be

categorized into two types: critical and noncritical equipment. Critical equipment are indispensable to keep the data center functioning. A typical design for critical equipment comprehends IT equipment and their supportive supply air fans in the CRAH. Noncritical equipment can be turned off for a short period of time without compromising the safety of the data center. They usually include all the other cooling equipment except CRAH supply air fans.

The data center is connected to the utility service and the backup generators at the building feeder. The incoming power is usually delivered to the data center building by a three-phase 480/277V AC system. During normal operation, the UPS is bypassed after it is fully charged. In emergency operation, before the backup generators are brought online, the UPS is only utilized to serve the critical equipment, and no power is delivered to the noncritical equipment.

The electrical system is modeled using the *Buildings.Electrical* package in the Modelica Buildings library. The UPS is modeled as a battery storage that does not consider the voltage and thermal dynamics during the charging and discharging process in this case, and is sized based on the selected critical equipment (IT equipment and supply air fan in the CRAH). The charging and discharging of the battery are controlled by the following logic shown in Figure 12. The state of charge (SOC) of a battery is its available capacity expressed as a percentage of its rated capacity. Knowing the SOC gives the user an indication of how long a battery will continue to perform before it is depleted. As it is not desired to deplete or overcharge the battery, the SOC of the battery should be kept within proper limits. Because the charging and discharging dynamics are not the purpose of this case study, we set the lower and upper bound of the SOC (SOC_l, and SOC_u) as 0 and 1, respectively. When connected to the utility or backup generators, the UPS is charged at a reference rate until being charged to SOC_u. When disconnected, the UPS discharges power to support critical equipment at a discharging rate of the minimum between the required rate $P_{dis,req}$

and the reference rate $P_{dis,ref}$. The potential voltage fluctuation during charging and discharging is not considered in this case.

```
if Connected then
    if SOC(t) < SOC_u then
        P_cha(t) ← P_cha,ref
    else
        P_cha(t) ← 0
    end if
else
    if SOC(t) < SOC_l then
        P_dis(t) ← 0
    else
        P_dis(t) ← min(P_dis,req, P_dis,ref)
    end if
end if
```

Figure 12. Pseudo codes of UPS charging and discharging control

4.2 Scenario 1: Normal Operation

Energy efficiency of the data center is considered as an important goal during normal operation. To quantify the energy efficiency, the Power Utilization Effectiveness $PUE = \frac{\int_{t_0}^{t_1} P_{feeder} dt}{\int_{t_0}^{t_1} P_{server} dt}$ is used, where P_{feeder} is the total power that are delivered into the data center for the IT equipment and all their supporting infrastructure, P_{server} is the power used only by the servers, and t_0 and t_1 is the start and the end time for calculating the PUE. The closer the PUE is to 1, the more efficient the data center is.

In this section, we investigate the different energy performances under different part load ratios (PLRs) of the cooling load in the data center room. The considered PLRs are 0.25, 0.50, 0.75 and 1.00, which represents the growing occupancy in the data center. The control settings for the cooling system in all PLRs are the same as the design condition as described in Section 4.1.1.

4.2.1 Simulation Results

Under design cooling load condition (PLR = 1.00), the breakdown of the annual electricity usage of the cooling system is shown in Figure 13. For the chilled water system with WSE, the economizing time, that is the period when the economizers are activated to pre-cool or fully cool the loads, is about 42% of the whole year (Figure 14). Because of the economizer operations, the fan in the CRAH is the major energy consumer, which takes up about 50.9% of total annual cooling energy. Chillers, pumps and cooling towers use 22.8%, 17.1% and 9.2%, respectively.

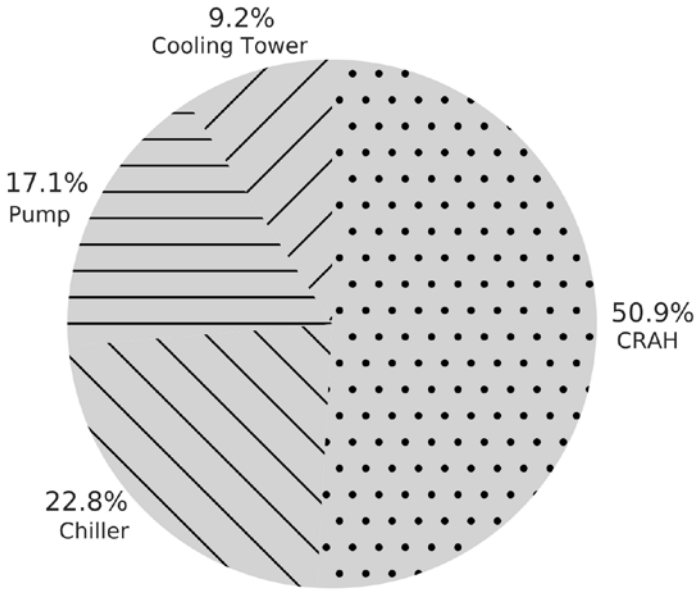

Figure 13. Breakdown of electricity usage of cooling system at PLR = 1.00

Figure 14(a) illustrates the normalized operation time of each cooling mode under different PLRs. As the PLR increases, the time when the cooling system stays in the FMC mode increases, and the time of the FC mode decreases. The time when the WSE is enabled decreases as the PLR increases. The cooling mode controller described in Section 3.3.1 takes as inputs weather conditions and temperatures in the chilled water loop and the condenser water loop. Although the same weather file is used under different PLRs, the return chilled water temperatures are different. For example,

the return chilled water temperature at PLR = 0.25 is higher than that at PLR = 1.00. Thus, condition (37) is faster to be triggered at PLR = 0.25 compared to PLR = 1.00, and hence the cooling system operates longer in the FC and the PMC mode at lower PLRs.

Figure 14(b) describes the relationship between PUEs and different PLRs. Among the four PLRs, the lowest PUE is 1.39 at PLR = 0.50, and hence maximum efficiency is achieved at part loads.

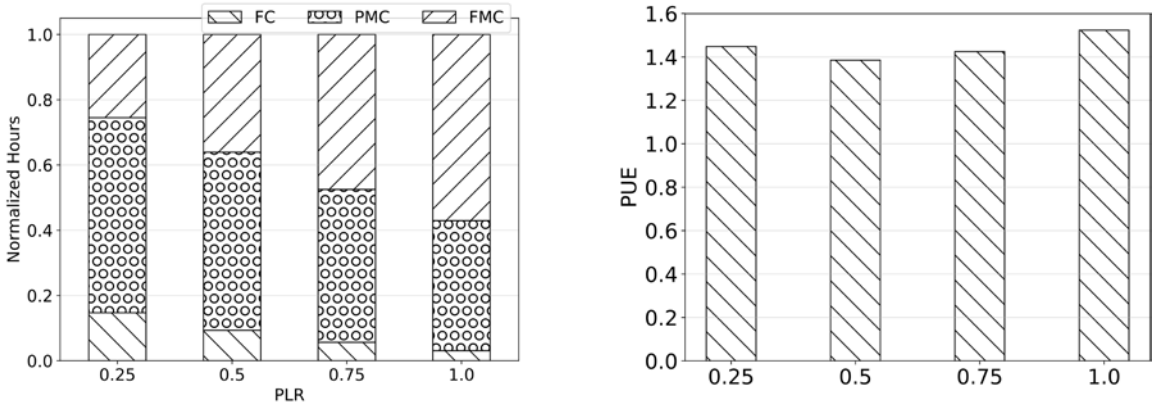

(a) Normalized hours (b) PUE

Figure 14. Operational status at different PLRs

Figure 15(a) shows the detailed energy consumption by each cooling component at different PLRs. The energy usage by the CRAH has an approximately cubic relationship with the PLR. The reason is when the supply and room air temperature control setpoints are not changed as the PLR changes, the speed of the fan in the CRAH is linear to the PLR in the room, and the fan power has a cubic relationship with its speed. Similar profile can be observed in the chilled water pumps. The energy consumption of the chiller has a weak quadratic relationship with the PLR, which is determined by the performance curves of the chillers and the hours of the PMC and FMC modes. Since the condenser water pumps have constant speed, the energy consumption is almost constant at PLR= 0.5, 0.75 and 1.00. A difference can be observed between PLR = 0.25 and other PLRs, because

only one condenser water pump is activated during the FMC mode when the PLR is 0.25, while two condenser water pumps are needed at other larger PLRs during the FMC mode. As for the cooling towers, the annual energy increases as the PLR increases, although the relative increase, compared with the fan in the CRAH, is small. The major reason is that the cooling system runs at the PMC mode during the most time of the year especially when the PLR is low, and the speed of the cooling tower fans in the PMC mode is set to 90% all the time.

Figure 15(b) plots the normalized energy for each cooling component divided by the current cooling load. The energy efficiency of the cooling tower fans and condenser water pumps increases as the PLR increases, while the opposite trends happen in the CRAH fan, chillers and chilled water pumps. The cooling system efficiency as a whole by combing all the cooling equipment is highest at PLR = 0.50. At that PLR, to address 1 kW of cooling load, the cooling system needs about 0.29 kW electricity.

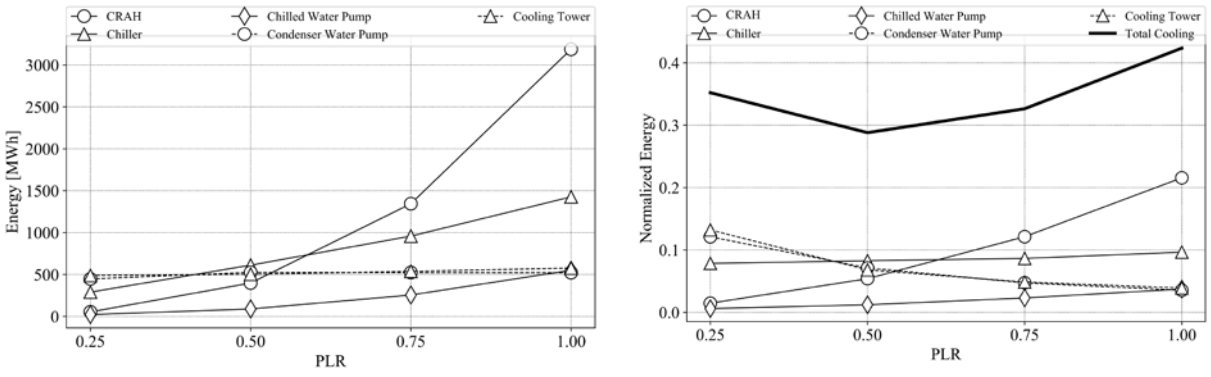

(a) Energy consumption (b) Normalized energy consumption

Figure 15. Detailed energy consumption in the cooling equipment

4.3 Scenario 2: Emergency Operation

The priority of emergency operation is to keep the data center safe. Thermally, safety means the heat generated by IT equipment can be removed timely to avoid the temperature of the IT equipment exceeding the maximum safety limit. Operation during emergency situations such as a blackout aims to maximize the use of the UPS by only powering critical equipment until backup generators are online. Given the capacity of the UPS, the selection of critical and noncritical equipment has significant influence on the survival time. Typically, in a chilled water system with WSE, critical equipment are the IT equipment and the fan in the CRAH. However, there may be opportunities to cool the data center with the UPS by considering some other cooling equipment as critical equipment when the outdoor air is cold enough to activate the WSE, especially when the data center is operating under part load. This scenario studies the impact of the selection of critical equipment in a chilled water system with WSE during emergency mode on the thermal and electrical performance in a data center under different cooling load and outdoor conditions.

4.3.1 Problem Formulation

The selection of the critical equipment in order to provide a thermally reliable environment even during the emergent gap can be formed as an optimization problem shown in (41).

$$\begin{aligned} \min \quad & E(s) = \int_{t1}^{t2} P(s,t)\, dt \\ s.t. \quad & T_{room}(s,t) \le T_{room,high} \\ & 0 < SOC(s,t) \le 1, \qquad t \in [t_1, t_2) \\ & SOC(s,t) \ge 0, \qquad t = t_2 \end{aligned} \tag{41}$$

The optimization goal in this case study is to minimize the usage of the UPS power E during the gap by choosing the best operation strategy s, although other goals can also be considered. One

constraint is that during the gap $t \in [t_1, t_2]$, the data center room temperature should not exceed a high limit $T_{room,high}$, because high temperature usually de-rates the power and IT equipment [33]. The other constraint is that the UPS must be able to support IT equipment during the gap, which means the SOC must be larger than zero before reaching the end of the gap.

Table 1. Operation strategies for emergency situations

Index	Strategy
s_1	The IT equipment and fan in the CRAHs are powered by the UPS during the 15-minute gap.
s_2	The IT equipment and all the cooling equipment other than the chillers are powered by the UPS during the 15-minute gap.
s_3	When the SOC in the UPS is greater than 0.5, then activate s_1. Otherwise activate s_2.

In this study, we assume that the power grid fails at $t_1 = 14{:}00$, and the gap ends at $t_2 = 14{:}15$. The high temperature limit is set to 35 °C. The power $P(s,t)$ is simulated using the Modelica models, and is integrated over t_1 to t_2. Three strategies (s_1, s_2 and s_3) for the selection of critical equipment are considered in this study, as shown in Table 1. The optimization problem is solved by exhaustively simulating and comparing the three operation strategies. The same optimization problem is also formulated and solved for different PLRs under different cooling modes. The results are detailed in the next section.

4.3.2 Simulation Results

(1) FC mode

The recommended emergent operation strategies for different PLRs under the FC mode is summarized in Table 2. Detailed explanations are shown in Figure 16 and illustrated as follows.

Table 2. Recommend emergent operation strategy for the FC mode under different PLRs

PLRs	s_1	s_2	s_3
0.25	x		
0.50		x	x
0.75		x	
1.00	x		

When the PLR is 0.25, s_1 performs better than s_2 and s_3 because it can keep the temperature within the high limit, and consumer the least energy from the UPS. The room temperature increases by 2.2 °C at the end of the power grid failure by utilizing s_1. The temperature rise is caused by the deactivation of cooling sources (chillers and economizers). On the contrary, the room temperature can be kept at 25 °C in s_2 and s_3 because the WSE is enabled to cool the room at the cost of more power drawn from the UPS. The SOC after 15 minutes in s_1 is 0.76, while that in s_2 and s_3 is 0.72. The SOC in s_2 and s_3 is the same because the SOC in this case is greater than 0.5 all the time, which makes s_3 the same as s_2. Compared with s_1, s_2 and s_3 consume less fan energy, because in s_2 and s_3 the fan speed is kept at around 0.25, while in s_1 the fan speed ramps up to around 0.85 in the 15 minutes because the fan needs to deliver more air to reduce the room temperature. For the discharging current (negative) in the UPS, s_1 discharges slower than s_2 and s_3 at the beginning. However, as the fan needs more energy in s_1, the UPS need discharge faster. Although s_1 requires more fan energy, the increased fan energy is still less than the energy required by the activation of more cooling equipment in s_2 and s_3.

When the PLR is 0.5, s_2 and s_3 have the same performance, and perform better than s_1, because they can maintain a lower room temperature and consume less energy from the UPS, although they power more equipment. In s_2 and s_3, the fan speed is maintained at 0.5 as in the normal operation,

while in s_3 the fan speed ramps up to 1 during the 15 minutes, which eventually leads to faster discharging and more energy consumption in the end.

When PLR is 0.75, s_2 performs better than s_1 and s_3, because it can lead to the lowest room temperature and consume the least energy. In s_1, the room temperature at the end of the gap increases to 33 °C. In s_2, the room temperature is still maintained at 25 °C. In s_3, the room temperature is kept at 25 °C before the first 10 minutes when the SOC of the UPS is greater than 0.5, and increases to 27 °C at the end of the failure. s_1 consumes more energy than s_2, because the fan in s_1 runs at the full speed during most of the gap. s_3 consumes slightly greater power than s_2 after the first 10 minutes because of the higher fan speed after deactivating the cooling equipment.

When PLR is 1.00, s_1 is the only strategy that can help the IT equipment survive 15 minutes, although the room temperature in the end reaches about 36 ^{o}C. For s_2, the room temperature is kept at 25 ^{o}C, but the UPS can only last about 13.5 minutes, which means the IT equipment has to be shut down for 1.5 minutes until the backup generators are on. Similarly, the UPS in s_3 can only last for 14.5 minutes. Though s_2 and s_3 can keep the data center room at a low temperature when data center is fully loaded, the reliability of the data center room is compromised.

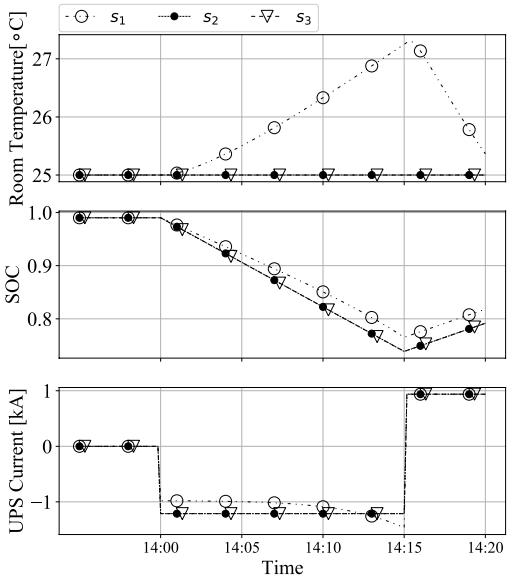

(a) PLR = 0.25

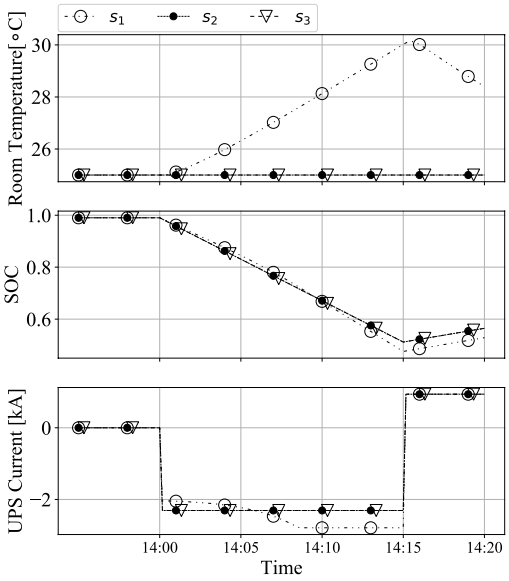

(b) PLR = 0.50

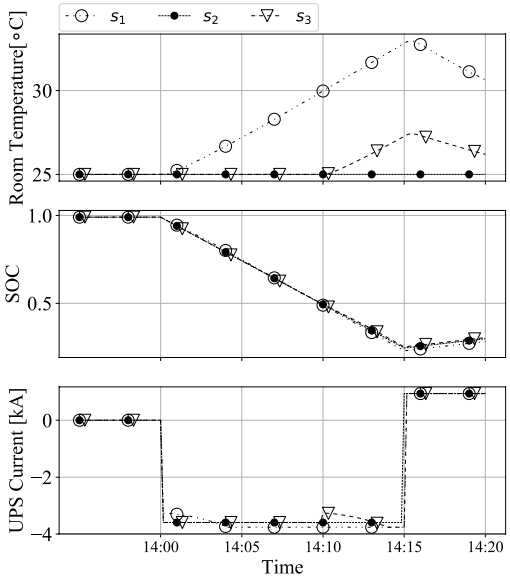

(c) PLR = 0.75

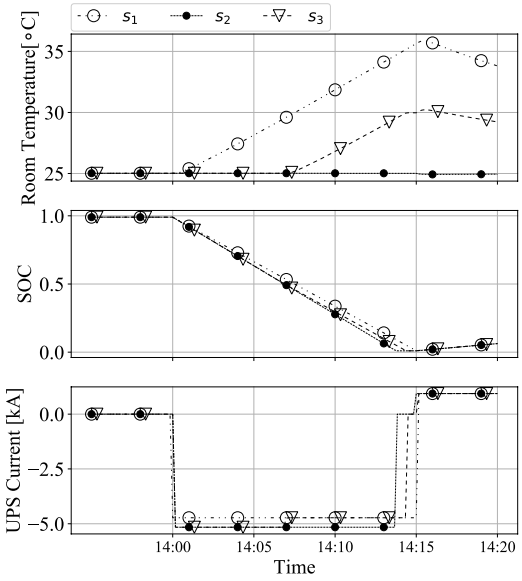

(d) PLR = 1.00

Figure 16. Comparison of blackout in the FC mode at four PLRs for different strategies

(2) FMC Mode

During the FMC mode, the waterside economizer is activated for emergency operation. In the 15 minutes, the outdoor air dry bulb temperature is around 28.5 ºC, and the wet bulb temperature is around 19.3 ºC. The economizer can take some heat out when the condenser water temperature is lower than that in the chilled water loop. Simulation results show that s_1 is the best strategy in the FMC mode for all PLRs.

As shown in Figure 17, s_1 outperforms s_2 and s_3 when PLR = 0.25, 0.50 and 0.75, because it consumes the least energy while maintaining the room temperature within the high limit. When PLR = 1.00, s_1 is the only strategy that depletes the UPS after the gap.

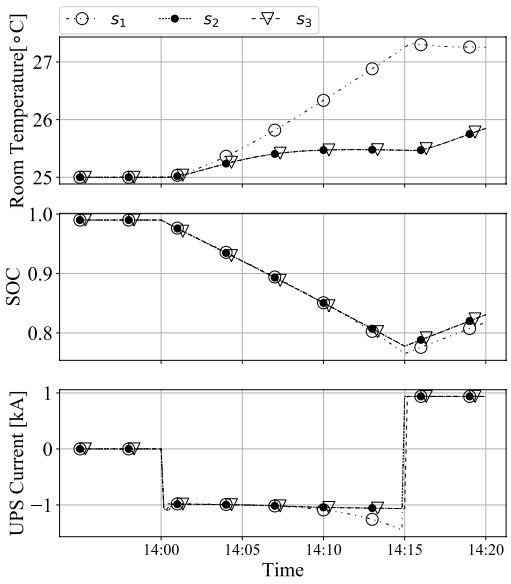

(a) PLR = 0.25

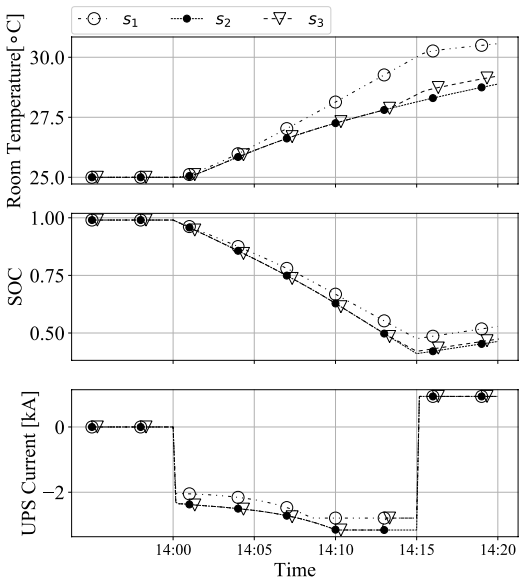

(b) PLR = 0.50

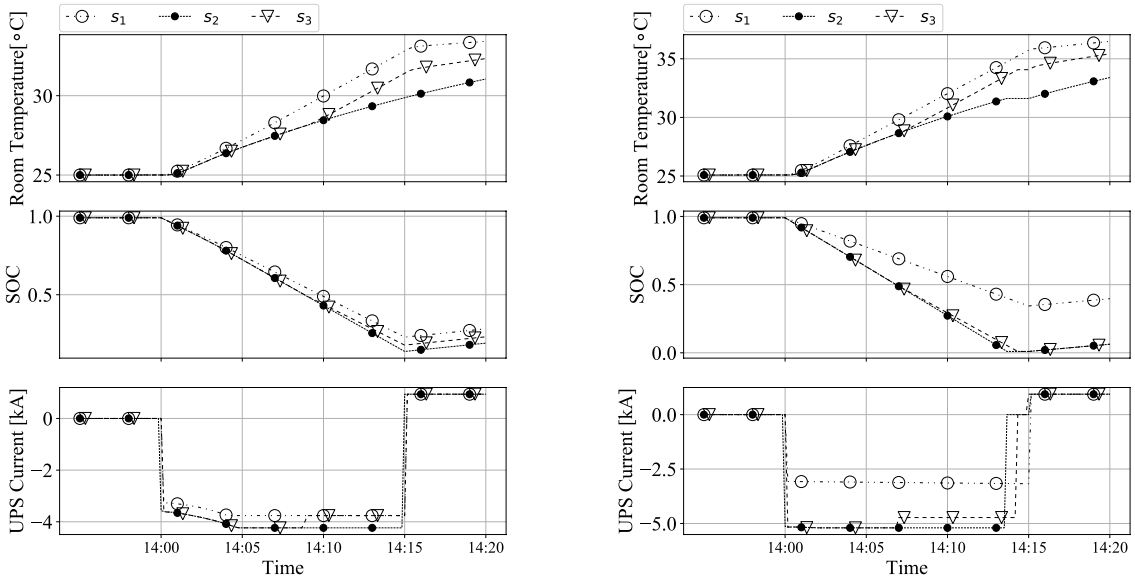

(c) PLR = 0.75 (d) PLR = 1.00

Figure 17. Comparison of blackout in the FMC mode at four PLRs for different strategies

5 Case Study 2: Renewable Data Center Operation

Data centers with renewable energy become increasingly attractive, especially for small and medium ones as their installations are cheaper and smaller. Renewable data centers can provide not only decent economical savings, but new opportunities to improve reliability due to the additional generation. This case study aims to investigate how the renewable data center behave under emergent situations with a special focus on how it can extend the survival time of the UPS.

The studied system is the same as case study 1, except that the data center is connected to an additional PV system. To quantify the impact of the PV to the data center, we introduce a

penetration factor r_{pv} that defines the ratio of the nominal power of the PV system to the nominal power of the data center. If r_{pv} is 0, then the data center cannot receive renewable power, and if r_{pv} is 1, the renewable energy can meet all the electrical demands in the data center at the nominal condition. To explore the survival time during emergency situation, we manually introduce a blackout at 12:00 pm, which lasts for 4 hours. The parameters r_{pv} and PLR are swept to show how the penetration of the PV system can affect the survival time of the UPS under different PLRs by using strategy s_2.

Figure 18 shows the lasting time of the UPS during FC and FMC mode for an emergency situation. Generally, as the penetration of renewable energy increases, the lasting time increases as well because more power can be drawn from the renewable sources and less from the UPS. For example, as shown in Figure 18(b), when the data center is running at a PLR of 0.75 in PMC mode, the UPS can only last about 16 minutes at no penetration, and about 211 minutes at a penetration of 0.8. Note that the maximum lasting time is 240 minutes because we only simulate a blackout for 4 hours. Therefore, the penetration of renewable energy in a data center can extend the lasting time of the UPS, thus increasing the data center reliability. The extra time may also be utilized when there are emergent system maintenances needed to be performed onsite.

The relationship between the lasting time and penetration of renewable energy is nonlinear. The nonlinearity is caused by the difference between the penetration and the PLR. If the penetration is higher than the PLR, the lasting time will increase significantly because the generation of renewable energy can meet the most or entire electrical demand in the data center, which thus requires little power from the UPS.

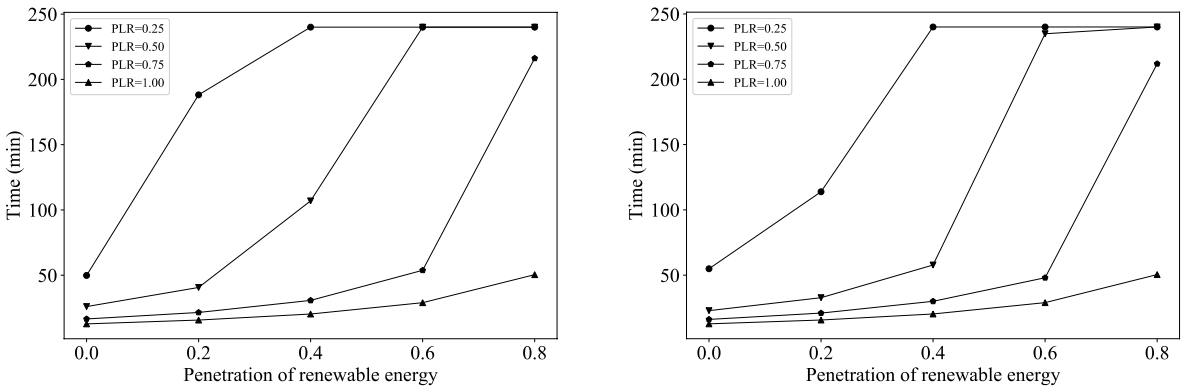

(a) FC mode (b) PMC mode

Figure 18. Comparison of UPS lasting time in a renewable data center at different cooling modes, PV penetration factors, and PLRs

Figure 19 compares the detailed SOC of the UPS and the current flows in two data centers with a penetration of 0 and 0.6. Without renewable resources, the UPS depletes after around 16 minutes. When the penetration of renewable resources increases to 0.6, the survival time can be extended to about 48 minutes. The SOC decreases non-smoothly when the PV system is penetrated, because of the oscillations of the PV current and the UPS current. The sharp changes in the PV current are due to the movement of clouds.

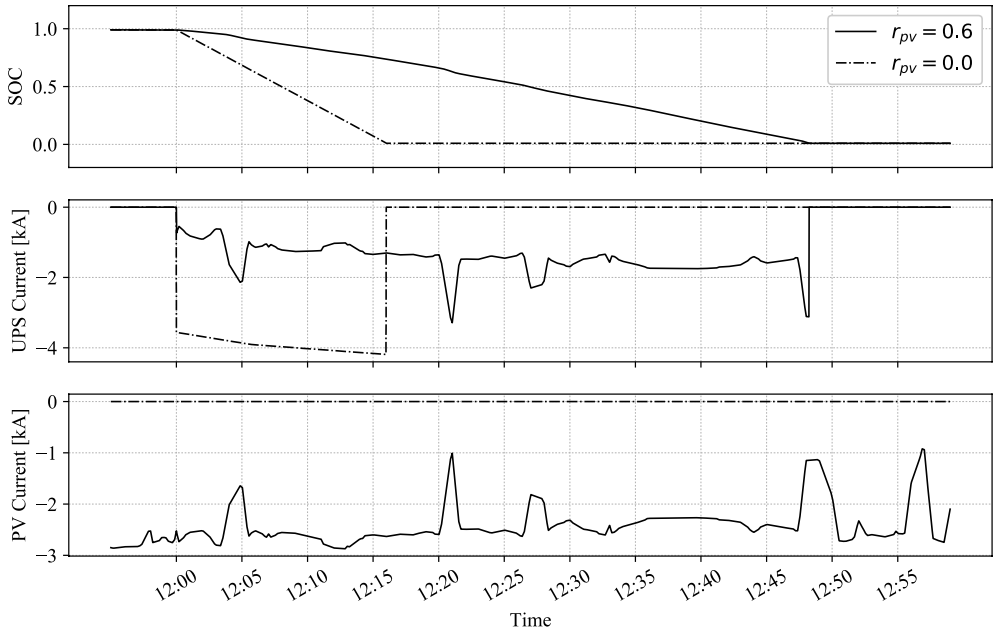

Figure 19. Comparison of detailed SOC and currents with and without PV

6 Conclusions

This paper presents an open source, equation-based, object-oriented Modelica package for data center cooling systems. This package includes major cooling component models, control logic, subsystem models and system templates for both chilled water system and direct expansion system, which are designed to support rapid virtual prototyping. The case studies show that this package is able to perform various analysis, including detailed analysis of energy efficiency and control performance in normal operation, as well as emergency operation. By integrating with the electrical models, detailed electrical analysis is also supported for both conventional and renewable data centers.

7 Acknowledgment

This research is financially funded by U.S. Department of Energy under the award NO. DE-EE0007688. This work was also supported by the Assistant Secretary for Energy Efficiency and Renewable Energy, the U.S. Department of Energy under Contract No. DE-AC02-05CH11231.

This work emerged from the IBPSA Project 1, an international project conducted under the umbrella of the International Building Performance Simulation Association (IBPSA). Project 1 will develop and demonstrate a BIM/GIS and Modelica Framework for building and community energy system design and operation.

8 Disclaimer

References

[1] J. Koomey, “Growth in data center electricity use 2005 to 2010,” *A report by Analytical Press, completed at the request of The New York Times*, vol. 9, 2011.

[2] W. Van Heddeghem, S. Lambert, B. Lannoo, D. Colle, M. Pickavet, and P. Demeester, “Trends in worldwide ICT electricity consumption from 2007 to 2012,” *Computer Communications*, vol. 50, pp. 64–76, 2014.

[3] K.-P. Lee and H.-L. Chen, “Analysis of energy saving potential of air-side free cooling for data centers in worldwide climate zones,” *Energy and Buildings*, vol. 64, pp. 103–112, 2013.

[4] Y. Pan, R. Yin, and Z. Huang, “Energy modeling of two office buildings with data center for green building design,” *Energy and Buildings*, vol. 40, no. 7, pp. 1145–1152, 2008.

[5] S.-W. Ham and J.-W. Jeong, “Impact of aisle containment on energy performance of a data center when using an integrated water-side economizer,” *Applied Thermal Engineering*, vol. 105, pp. 372–384, 2016.

[6] A. Agrawal, M. Khichar, and S. Jain, “Transient simulation of wet cooling strategies for a data center in worldwide climate zones,” *Energy and Buildings*, vol. 127, pp. 352–359, 2016.

[7] A. Shehabi *et al.*, “Energy implications of economizer use in california data centers,” 2008.

[8] M. Wetter, “Modelica-based modelling and simulation to support research and development in building energy and control systems,” *Journal of Building Performance Simulation*, vol. 2, no. 2, pp. 143–161, 2009.

[9] Y. Fu, M. Wetter, and W. Zuo, “Modelica models for data center cooling systems,” in *2018 Building Performance Analysis Conference and SimBuild, Chicago, Illinois, United States of America*, 2018.

[10] M. Wetter, M. Bonvini, and T. S. Nouidui, “Equation-based languages – A new paradigm for building energy modeling, simulation and optimization,” *Energy and Buildings*, vol. 117, pp. 290–300, 2016.

[11] V. V. G. Krishnan, Y. Zhang, K. Kaur, A. Hahn, A. Srivastava, and S. Sindhu, “Cyber-Security Analysis of Transactive Energy Systems,” in *2018 IEEE/PES Transmission and Distribution Conference and Exposition (T D)*, 2018, pp. 1–9.

[12] H. Elmqvist, S. E. Mattsson, and M. Otter, “Modelica: The new object-oriented modeling language,” in *12th European Simulation Multiconference, Manchester, UK*, 1998.

[13] M. Otter, K.-E. Årzén, and I. Dressler, “StateGraph-a Modelica library for hierarchical state machines,” *Modelica 2005 proceedings*, 2005.

[14] M. Wetter, W. Zuo, T. S. Nouidui, and X. Pang, “Modelica buildings library,” *Journal of Building Performance Simulation*, vol. 7, no. 4, pp. 253–270, 2014.

[15] B. Eisenhower, K. Gasljevic, and I. Mezi, “Control-Oriented Dynamic Modeling and Calibration of a Campus Theater Using Modelica,” *Proceedings of SimBuild*, vol. 5, no. 1, pp. 112–119, 2012.

[16] Y. Fu, W. Zuo, M. Wetter, J. W. VanGilder, X. Han, and D. Plamondon, “Equation-Based object-oriented modeling and simulation for data center Cooling: A case study,” *Energy and Buildings*, vol. 186, pp. 108–125, 2019.

[17] Y. Fu, S. Huang, D. Vrabie, and W. Zuo, “Coupling Power System Dynamics and Building Dynamics to Enabling Building-to-Grid Integration,” in *Proceedings of the 13th International Modelica Conference, Regensburg, Germany, March 4--6, 2019*, 2019, no. 157.

[18] Y. Fu, X. Lu, and W. Zuo, “Modelica Models for the Control Evaluations of Chilled Water System with Waterside Economizer,” in *Proceedings of the 13th International Modelica Conference, Regensburg, Germany, March 4--6, 2019*, 2019, no. 157.

[19] M. Wetter, “A Modelica-based model library for building energy and control systems,” in *Proceedings of the 11th IBPSA Conference, Glasgow, Scotland*, 2009, pp. 652–659.

[20] D. Lee, B. Lee, and J. W. Shin, “Fault detection and diagnosis with modelica language using deep belief network,” in *Proceedings of the 11th International Modelica Conference, Versailles, France, September 21-23, 2015*, 2015, no. 118, pp. 615–623.

[21] S. Huang, W. Zuo, and M. D. Sohn, “Amelioration of the cooling load based chiller sequencing control,” *Applied Energy*, vol. 168, pp. 204–215, 2016.

[22] S. Huang, W. Zuo, and M. D. Sohn, “Improved cooling tower control of legacy chiller plants by optimizing the condenser water set point,” *Building and Environment*, vol. 111, pp. 33–46, 2017.

[23] W. Tian, Y. Fu, Q. Wang, T. A. Sevilla, and W. Zuo, “Optimization on Thermostat Location in an Office Room Using the Coupled Simulation Platform in Modelica Buildings Library: A Pilot Study,” in *2018 COBEE conference*, 2018.

[24] W. Tian, T. A. Sevilla, W. Zuo, and M. D. Sohn, “Coupling fast fluid dynamics and multizone airflow models in Modelica Buildings library to simulate the dynamics of HVAC systems,” *Building and Environment*, vol. 122, pp. 269–286, 2017.

[25] K. Ebrahimi, G. F. Jones, and A. S. Fleischer, “A review of data center cooling technology, operating conditions and the corresponding low-grade waste heat recovery opportunities,” *Renewable and Sustainable Energy Reviews*, vol. 31, pp. 622–638, 2014.

[26] C. B. Bash, C. D. Patel, and R. K. Sharma, “Dynamic thermal management of air cooled data centers,” in *Thermal and Thermomechanical Proceedings 10th Intersociety Conference on Phenomena in Electronics Systems, 2006. ITHERM 2006.*, 2006, pp. 445–

452.

[27] U. S. DoE, “Energyplus engineering reference,” *The reference to energyplus calculations*, 2016.

[28] ASHRAE, *ASHRAE HandBook: HVAC systems and equipment*. 2016.

[29] J. Stein, “Waterside Economizing in Data Centers: Design and Control Considerations.,” *ASHRAE Transactions*, vol. 115, no. 2, 2009.

[30] S. T. Taylor, “How to design & control waterside economizers,” *ASHRAE Journal*, vol. 56, no. 6, pp. 30–36, 2014.

[31] Z. M. Pardey, D. W. Demetriou, H. S. Erden, J. W. VanGilder, H. E. Khalifa, and R. R. Schmidt, “Proposal for standard compact server model for transient data center simulations,” *ASHRAE Transactions*, vol. 121, no. 1, pp. 413–422, 2015.

[32] M. Sun, Y. Xue, P. Bogdan, J. Tang, Y. Wang, and X. Lin, “Hierarchical and hybrid energy storage devices in data centers: Architecture, control and provisioning,” *PloS one*, vol. 13, no. 1, p. e0191450, 2018.

[33] ASHRAE, *Thermal guidelines for data processing environments*, 4th ed. 2015.